Well-posedness of an evaporation model for a spherical droplet exposed to an air flow

Eberhard Bänsch, Martin Doß, Carsten Gräser, and Nadja Ray

Abstract. In this paper, we address the well-posedness of an evaporation model for a spherical liquid droplet taking into account the convective impact of an air flow in the ambient gas phase. From a mathematical perspective, we are dealing with a coupled ODE–PDE system for the droplet radius, the temperature distribution, and the vapor concentration. The nonlinear coupling arises from the evaporation rate modeled by the Hertz–Knudsen equation. Under physically meaningful assumptions, we prove existence and uniqueness of a weak solution until the droplet has evaporated completely. Numerical simulations are performed to illustrate how different air flows affect the evaporation process.

1. Introduction

Evaporation plays an important role in a variety of practical applications ranging from weather forecasting [36] to the production of pharmaceutical powders [34]. If convective currents complicate the temperature and vapor mass distributions, it is particularly important to understand their impact on the evaporation process. Mathematical models can be powerful tools to unravel the complex physics behind convective evaporation provided that the heat and mass fluxes across the liquid–gas interface are captured correctly. Depending on the characteristic length and time scales, there are two different modeling approaches: if the volatile liquid evaporates slowly, one usually assumes thermodynamic equilibrium in the sense that the saturated vapor pressure equals the actual vapor pressure at the liquid–gas interface. In general, however, the saturated and the actual vapor pressure do not coincide and their difference determines the evaporation rate. Taking into account this imbalance, nonequilibrium evaporation models are physically more accurate. The Hertz–Knudsen equation is especially widely used to model and simulate evaporation [19]. As a nonlinear boundary condition, it couples the heat and mass transfer within and around the volatile liquid. Among all possible applications, the evaporation of small droplets was found to be especially well described by the Hertz–Knudsen equation (see [39]). Our aim is to study the mathematical well-posedness of the related evaporation model for a single droplet taking into account the convective impact of an air flow in the ambient gas phase.

The following literature is related to our problem: first of all, the quasi-stationary evaporation of a spherical droplet into stagnant air is well described analytically by the d^2 law. As suggested by its name, the d^2 law states that the squared diameter (or radius) of the droplet decreases linearly with time [22]. The same behavior follows from the model in [2], which also accounts for nonequilibrium effects. From a mathematical perspective, single droplet evaporation (and condensation) can be regarded as a generalized Stefan problem [14]. The latter is widely known to be well-posed in one and more spatial dimensions [11, 15, 30, 35]. The main difference between single droplet evaporation and the classical Stefan problem arises from the fact that the saturated vapor pressure depends on the temperature at the droplet surface, which is neglected in [14]. The authors of [28, 29] consider a more general model for two-phase flow with phase transition derived from the balances of mass, momentum, and energy in a thermodynamically consistent way. Their existence result applies to nearly flat interfaces and small initial data. It should be mentioned that the interface laws for evaporation (and condensation) are very similar to the ones for alloy solidification, as reviewed in [6]. Finally, the cell problems whose well-posedness is also studied in [16] are closely related to our topic despite their application being different. Since the upscaled model in [16] describes mineral dissolution and precipitation in a porous medium, each cell represents a single spherical grain whose radius is governed by a nonlinear ordinary differential equation. More general cell geometries are studied in [17] using a level-set approach to prove the stability of the corresponding diffusion and permeability tensors. Even if the interface conditions for mineral dissolution and droplet evaporation appear to be similar, it should be pointed out that the latter are generally more complicated. While dissolution can be regarded as an isothermal process, evaporation causes a discontinuity of the normal heat flux which is commonly known as evaporative cooling. Therefore, the evaporation rate determines both the mass and the heat flux across the liquid–gas interface.

Our aim is to study the mathematical well-posedness of a nonequilibrium evaporation model for a single spherical droplet which is exposed to an air flow in the ambient gas phase. The considered evaporation model consists of an ordinary differential equation for the droplet radius and two convection–diffusion equations for the temperature and vapor mass distributions. The mathematical challenges of the resulting ODE–PDE system mainly arise from its nonlinear coupling at the droplet surface and the evolution of the latter as a free boundary. More precisely, the evaporation rate is computed from the thermodynamic nonequilibrium between the saturated and the actual vapor pressure at the droplet surface via the Hertz–Knudsen equation. To handle the resulting nonlinear boundary condition for the heat and vapor mass flux, we apply the method of upper and lower solutions. Regarding the radius of the droplet as its time-dependent characteristic length, we rescale our model accordingly to immobilize the free phase boundary. By that, the interface velocity can be treated as an additional flux term in the transport equations for the temperature and vapor mass distributions. Finally, we apply Banach's fixed-point theorem to prove the existence of a unique weak solution and show stability with respect to perturbations of the initial values.
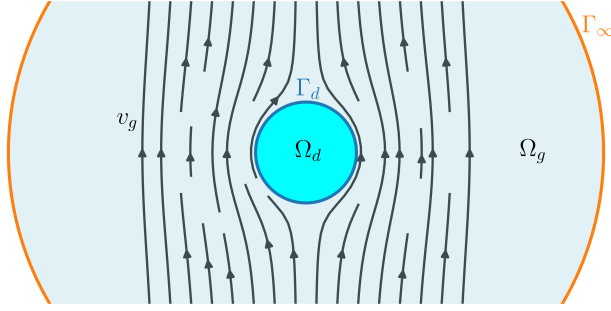
Figure 1. Schematic illustration of the evaporating droplet exposed to an air flow.

The paper is structured as follows: in Section 2, we introduce our mathematical model for the convective evaporation of a single droplet. In Section 3, the latter is shown to admit a unique maximal weak solution as outlined above. The numerical simulations performed in Section 4 illustrate the convective impact of the ambient air flow on the evaporation rate. Finally, Section 5 concludes our paper.

2. Droplet evaporation model

In this section, we present our mathematical model for the convective evaporation of a single spherical droplet exposed to an air flow in the ambient gas phase. As illustrated in Figure 1, the droplet surface is denoted by $\Gamma_d := \partial\Omega_d$, while $\Omega_d \subset \mathbb{R}^3$ represents its liquid interior. The total droplet volume $V_d := |\Omega_d|$ is then governed by the ordinary differential equation

$$\rho_d \frac{dV_d}{dt} = -\int_{\Gamma_d} J \, d\sigma, \tag{2.1}$$

with the mass density ρ_d of the volatile liquid and the evaporation rate J per surface area. The ambient gas phase Ω_g is usually not stagnant. In many practical applications, either natural or forced convection can have a significant impact on the evaporation process. Let v_g be the corresponding velocity field and n the outer unit normal of the gas phase. Likewise, the velocity field v_d describes the convection inside the liquid droplet. Both velocity fields are assumed to be given. Further assuming v_d and v_g to be quasi-stationary, we require

$$v_d \cdot n = 0 \quad \text{and} \quad v_g \cdot n = 0 \quad \text{on } \Gamma_d \tag{2.2}$$

for the sake of simplicity. In other words, there is no convective flux across the droplet surface. The heat and vapor mass transport is then governed by the following system of

convection–diffusion equations:

$$\rho_d C_{p,d} \partial_t T_d = \nabla \cdot (k_d \nabla T_d - \rho_d C_{p,d} T_d v_d) \quad \text{in } \Omega_d, \tag{2.3}$$

$$\rho_g C_{p,g} \partial_t T_g = \nabla \cdot (k_g \nabla T_g - \rho_g C_{p,g} T_g v_g) \quad \text{in } \Omega_g, \tag{2.4}$$

$$\partial_t \rho_v = \nabla \cdot (D_v \nabla \rho_v - \rho_v v_g) \quad \text{in } \Omega_g, \tag{2.5}$$

subject to the interface flux conditions

$$(k_g \nabla T_g - k_d \nabla T_d) \cdot n = -\Lambda J \quad \text{on } \Gamma_d, \tag{2.6}$$

$$D_v \nabla \rho_v \cdot n = J \quad \text{on } \Gamma_d, \tag{2.7}$$

where ρ_g denotes the total mass density of the gas phase, ρ_v the vapor mass density, $T_{d/g}$ the droplet/gas temperature, $C_{p,d/g}$ the respective specific heat capacity, $k_{d/g}$ the respective thermal conductivity, D_v the vapor diffusion coefficient, and Λ the specific latent heat of vaporization. The continuity of temperature naturally implies $T_d = T_g$ on Γ_d which serves as an additional boundary condition.

The evaporation rate J is modeled by the Hertz–Knudsen equation. It relates J to the thermodynamic nonequilibrium between the saturated and the actual vapor pressure at the liquid–gas interface. In its original formulation, the Hertz–Knudsen equation reads as follows [19]:

$$J = \sqrt{\frac{M_d}{2\pi \mathcal{R} T_d}} (p_{\text{sat}} - p_v), \tag{2.8}$$

with the molar mass M_d of the volatile liquid, the ideal gas constant $\mathcal{R}$, the droplet temperature T_d, the saturated vapor pressure p_{sat}, and the actual vapor pressure p_v at the liquid–gas interface. It should be mentioned that (2.8) models both evaporation ($J \geq 0$) and condensation ($J \leq 0$) depending on the relative humidity $\text{RH} := p_v / p_{\text{sat}}$ at the droplet surface. Further notice that p_v and ρ_v are related to each other via the ideal gas law $p_v M_d = \rho_v \mathcal{R} T_g$. The saturated vapor pressure, on the other hand, is determined by the interface temperature via the Clausius–Clapeyron relation. In the case of water, the latter is well approximated by the Tetens equation [25]

$$\frac{p_{\text{sat}}}{610.78\,\text{Pa}} = \exp\left(\frac{17.27\,T_g}{T_g + 237.3\,°\text{C}}\right), \tag{2.9}$$

with T_g in degrees Celsius. Far away from the droplet, the temperature and vapor mass distributions are supposed to be consistent with the drying conditions. Their radial limits are given by

$$\lim_{|x|\to\infty} T_g(t, x) = T_\infty \quad \text{and} \quad \lim_{|x|\to\infty} \rho_v(t, x) = \rho_\infty, \tag{2.10}$$

where T_∞ denotes the temperature and ρ_∞ the vapor mass density of the drying air. It should be pointed out that T_∞ and ρ_∞ are both regarded as constants.

The presented evaporation model is highly relevant for a plethora of practical applications, such as spray drying or air conditioning [33]. However, to the best of our knowledge, its mathematical well-posedness has not yet been verified in the existing literature. In this paper, we show existence and uniqueness of a weak solution under the following assumptions and simplifications:

A1. Neglecting possible deformations due to external forces such as drag, the droplet remains spherical throughout its evaporation process. This simplification is motivated by the fact that surface tension usually dominates if the droplet is sufficiently small. The evolution of the droplet radius R_d over time is then governed by the ordinary differential equation

$$\rho_d \frac{dR_d}{dt} = -\frac{1}{4\pi R_d^2} \int_{\Gamma_d} J \, d\sigma, \tag{2.11}$$

which follows from (2.1) by inserting the formula $V_d = 4/3\pi R_d^3$ for the droplet volume.

A2. As illustrated in Figure 1, the ambient gas phase Ω_g is truncated far away from the droplet such that its rescaled domain $\Omega_g^* := \Omega_g / R_d$ becomes a spherical shell with fixed boundaries.

A3. The drying conditions are sufficiently moderate such that thermal variations inside the droplet can be neglected. More precisely, we assume $k_d \nabla T_d \cdot n \approx 0$ in interface condition (2.6) for the normal heat flux across the droplet surface. According to [27], this is only the case if the Biot number[1] of the evaporation process is sufficiently small. In other words, the evaporation process lasts significantly longer than the initial convergence of T_d towards the wet-bulb temperature[2].

A4. The Hertz–Knudsen equation (see (2.8)) for the evaporation rate is approximated as follows:

$$J = \sqrt{\frac{\mathcal{R} T_g}{2\pi M_d}} (\rho_{\text{sat}} - \rho_v) \approx C(\rho_{\text{sat}} - \rho_v), \tag{2.12}$$

neglecting the temperature dependence of $C > 0$ and simply regarding it as a positive constant. Motivated by the Tetens equation (see (2.9)), the saturated vapor mass density $\rho_{\text{sat}} := p_{\text{sat}} M_w / (\mathcal{R} T_g)$ is assumed to admit a continuous derivative with respect to the gas temperature satisfying

$$0 \le \frac{d\rho_{\text{sat}}}{dT_g} \le L \tag{2.13}$$

for some Lipschitz constant $L > 0$.

---

[1]The Biot number is defined as $\text{Bi} = h R_d / k_d$, where h denotes the heat transfer coefficient across the droplet surface.

[2]The wet-bulb temperature is defined as the temperature measured by a thermometer whose bulb is covered by a wet cloth [7]. Its constant value is uniquely determined by the drying conditions.

A5. As we are concerned with evaporation, the relative humidity of the drying air fulfills RH $\leq 100\,\%$ far away from the droplet. Consequently, the drying conditions satisfy $\rho_\infty \leq \rho_{\text{sat}}(T_\infty) =: \rho_*$ and there exists a temperature $T_* \leq T_\infty$ such that the corresponding saturated vapor mass density equals $\rho_{\text{sat}}(T_*) = \rho_\infty$. Be aware that droplet condensation ($\rho_\infty > \rho_{\text{sat}}(T_\infty)$) is not studied for the ease of presentation. It should, however, be mentioned that the corresponding mathematical problem can be addressed in a similar manner if some signs and inequalities (e.g., in (3.2) or Proposition 1) are switched accordingly.

A6. The air flow is described by a quasi-stationary incompressible velocity field $v_g \in H^1(\Omega_g, \mathbb{R}^3)$ which is assumed to be given. More precisely, it satisfies $\nabla \cdot v_g = 0$ in Ω_g and $v_g \cdot n = 0$ on Γ_d. The velocity field $v_g = v_g(R_d)$ depends continuously on the droplet radius R_d in the following sense: for each $\eta > 0$, there exists a Lipschitz constant $L_\eta > 0$ such that

$$\sup_{x \in \Omega_g^*} |v_g^1(xR_d^1) - v_g^2(xR_d^2)| \leq L_\eta |R_d^1 - R_d^2| \tag{2.14}$$

holds for all droplet radii $R_d^1, R_d^2 > \eta$, where v_g^1 and v_g^2 denote the corresponding velocity fields for the air flow in the ambient gas phase. In other words, the rescaled velocity field v_g^* defined below is uniquely determined by the droplet radius R_d and (2.14) guarantees the Lipschitz continuity of the mapping $R_d \mapsto v_g^* \in L^\infty(\Omega_g^*; \mathbb{R}^3)$ if the droplet radius R_d is bounded away from zero.

A7. Without loss of generality, all physical constants are assumed to be one for the ease of presentation. However, keep in mind that T_g and ρ_v do not satisfy the same convection–diffusion equation in the sense that their coefficients are different!

Regarding the radius R_d of the droplet as its time-dependent characteristic length, we rescale our model accordingly. Define $x^* := x/R_d \in \Omega_g^*$ for all spatial coordinates $x \in \Omega_g$. The time derivatives of the gas temperature T_g and its rescaled counterpart $T_g^*(t, x^*) := T_g(t, x)$ are then related to each other via

$$\partial_t T_g(t, x) = \partial_t T_g^*(t, x^*) + \nabla^* T_g^*(t, x^*) \cdot \partial_t x^*$$
$$= \partial_t T_g^*(t, x^*) - \frac{\dot{R}_d}{R_d} \nabla^* T_g^*(t, x^*) \cdot x^*, \tag{2.15}$$

where $\nabla^* = R_d \nabla$ denotes the rescaled spatial gradient. Notice that (2.15) follows directly from the chain rule. The same identity holds for the rescaled counterpart $\rho_v^*(t, x^*) := \rho_v(t, x)$ of the vapor mass density. Altogether, the rescaled simplified version of our single droplet evaporation model whose well-posedness will be studied in Section 3 reads as follows:

$$\dot{R}_d = -\frac{1}{4\pi} \int_{\Gamma_d^*} J(T_g^*, \rho_v^*) \, d\sigma, \tag{E1}$$

$$\partial_t T_g^* = \frac{1}{R_d^2} \Delta^* T_g^* - \frac{1}{R_d} \nabla^* T_g^* \cdot (v_g^* - \dot{R}_d x^*) \quad \text{in } \Omega_g^*, \tag{E2}$$

$$\partial_t \rho_v^* = \frac{1}{R_d^2} \Delta^* \rho_v^* - \frac{1}{R_d} \nabla^* \rho_v^* \cdot (v_g^* - \dot{R}_d x^*) \quad \text{in } \Omega_g^*, \tag{E3}$$

$$\frac{1}{R_d} \nabla^* T_g^* \cdot n^* = -J(T_g^*, \rho_v^*) \qquad \qquad \text{on } \Gamma_d^*, \tag{E4}$$

$$\frac{1}{R_d} \nabla^* \rho_v^* \cdot n^* = J(T_g^*, \rho_v^*) \qquad \qquad \text{on } \Gamma_d^*, \tag{E5}$$

$$T_g^* = T_\infty \qquad \qquad \text{on } \Gamma_\infty^*, \tag{E6}$$

$$\rho_v^* = \rho_\infty \qquad \qquad \text{on } \Gamma_\infty^* \tag{E7}$$

with the Nemytskii operator $J(T_g^*, \rho_v^*) := \rho_{\text{sat}}(T_g^*) - \rho_v^*$ for the evaporation rate. Recall that the boundaries $\Gamma_d^* := \{x^* \in \mathbb{R}^3 : |x^*| = 1\}$ and $\Gamma_\infty^* = \partial \Omega_g^* \setminus \Gamma_d^*$ of the rescaled gas phase are now fixed. In return, the interface velocity now appears in the transport equations of our model. For the ease of presentation, the sub- and superscripts 'd', 'g', 'v', and '$*$' will be omitted in what follows.

3. Well-posedness of the droplet evaporation model

In this section, we show that the presented droplet evaporation model (E1)–(E7) admits a unique weak solution taking into account assumptions (A1)–(A7) from above. From a mathematical perspective, we are dealing with a coupled ODE–PDE system for the droplet radius, the temperature distribution, and the vapor mass concentration. The non-linear coupling arises from the evaporation rate being modeled by the Hertz–Knudsen equation.

As mentioned above, the well-posedness of our single droplet evaporation model will be studied in the context of weak solutions. The underlying Lebesgue and Sobolev spaces are denoted by $L^2(\Omega)$ and $H^1(\Omega) = W^{1,2}(\Omega)$, respectively. Let $\langle \cdot, \cdot \rangle$ be the pairing of $X := \{\varphi \in H^1(\Omega) : \varphi = 0 \text{ on } \Gamma_\infty\}$ and its dual space X^*. The droplet evaporation problem whose governing equations and boundary conditions (E1)–(E7) were derived in Section 2 admits the following weak formulation:

Definition 1 (Weak solution of the droplet evaporation problem). Let $R_0 > 0$ and T_0, $\rho_0 \in L^2(\Omega)$ be given. The triple (R, T, ρ) is called a weak solution of the droplet evaporation problem given by (E1)–(E7) if

- $R \in H^1(I)$ satisfies $R(0) = R_0$ and the evolution equation

$$\dot{R}(t) = -\frac{1}{4\pi} \int_\Gamma J(T, \rho) \, d\sigma \quad \text{with} \quad J(T, \rho) = \rho_{\text{sat}}(T) - \rho \tag{P1}$$

for almost every $t \in I$,

- $T, \rho \in L^2(I, H^1(\Omega))$ with $\partial_t T, \partial_t \rho \in L^2(I, X^*)$ satisfy the weak formulations

$$\langle \partial_t T, \varphi \rangle + \int_\Omega \frac{1}{R^2} \nabla T \cdot \nabla \varphi + \frac{1}{R} \nabla T \cdot [v(R) - \dot{R}x] \varphi \, dx + \frac{1}{R} \int_\Gamma J(T, \rho) \varphi \, d\sigma$$
$$= 0, \tag{P2}$$

$$\langle \partial_t \rho, \varphi \rangle + \int_\Omega \frac{1}{R^2} \nabla \rho \cdot \nabla \varphi + \frac{1}{R} \nabla \rho \cdot [v(R) - \dot{R}x] \varphi \, dx - \frac{1}{R} \int_\Gamma J(T, \rho) \varphi \, d\sigma$$
$$= 0 \tag{P3}$$

for all test functions $\varphi \in X$,

- the initial and drying conditions

$$T(0) = T_0 \quad \text{and} \quad \rho(0) = \rho_0 \quad \text{in } \Omega, \tag{P4}$$
$$T = T_\infty \quad \text{and} \quad \rho = \rho_\infty \quad \text{on } \Gamma_\infty \tag{P5}$$

are fulfilled.

As formulated in Theorem 3, our main result will be the existence of a unique weak solution in the sense of Definition 1 until the droplet has evaporated completely. Formally speaking, the strategy of our proof can be outlined as follows: first, we consider the droplet radius to be given and show that the decoupled evaporation problem given by (P3)–(P5) admits a unique weak solution. In Proposition 2, the resulting solution operator $S(R)$ $:= (T, \rho)$ is shown to be Lipschitz continuous. The coupled ODE–PDE system (P1)–(P5) with unknown droplet radius is then reformulated as a fixed-point problem. Notice that R is a fixed-point of the Volterra operator

$$\mathcal{T}(R)(t) := R_0 - \frac{1}{4\pi} \int_0^t \int_\Gamma J(S(R)) \, d\sigma \, d\tau \tag{3.1}$$

if (R, T, ρ) is a weak solution of the droplet evaporation problem. On the other hand, if $R \in H^1(I)$ satisfies $\mathcal{T}(R) = R$, then $(R, S(R))$ solves the droplet evaporation problem in the sense of Definition 1. Therefore, finding a solution to the latter is equivalent to a fixed-point problem. In Section 3.3, we show that $\mathcal{T}$ is a well-defined contraction on the following set of admissible droplet radii:

$$\Sigma_{t_*} := \{ R \in H^1(I) \, : \, R(0) = R_0 \text{ and } |\dot{R}(t)| \leq J(T_\infty, \rho_\infty) \text{ for a.e. } t \in I \}, \tag{3.2}$$

provided that the underlying time interval $I := [0, t_*)$ is sufficiently small. The existence of a fixed-point $R \in \Sigma_{t_*}$ with $\mathcal{T}(R) = R$ then follows from Banach's fixed-point theorem. Finally, we show that the time interval I of the weak solution can be extended until the droplet has evaporated completely.

3.1. Preliminaries

Throughout the entire paper, the constant $C > 0$ is meant to be generic in the sense that its value can be redefined. Unless stated otherwise, it only depends on constant coefficients

and the spatial domain Ω of our model, but not on the time interval I of its solution. For the ease of presentation, we define $\| \cdot \|_{2,\Omega} := \| \cdot \|_{L^2(\Omega)}$ to abbreviate the $L^2(\Omega)$-norm. The following interpolation inequality will be instrumental to handle boundary terms:

Lemma 1. *Let $\Omega \subset \mathbb{R}^3$ be a bounded C^2-domain. Then, $u \in H^1(\Omega)$ satisfies*

$$\|u\|_{2,\partial\Omega}^2 \leq \varepsilon \|\nabla u\|_{2,\Omega}^2 + \frac{C}{\varepsilon} \|u\|_{2,\Omega}^2 \tag{3.3}$$

for all $\varepsilon \in (0,1)$. The constant $C > 0$ only depends on Ω.

From [18, Lemma 7.9], we adopt the following proof:

Proof. First of all, the continuity of the trace operator [1, Theorem 7.58] implies

$$\|u\|_{2,\partial\Omega} \leq C \|u\|_{H^{1/2}(\Omega)} \tag{3.4}$$

for some $C > 0$. From $H^1(\Omega) \hookrightarrow H^{1/2}(\Omega) \hookrightarrow L^2(\Omega)$ we infer the interpolation inequality

$$\|u\|_{H^{1/2}(\Omega)}^2 \leq C \|u\|_{H^1(\Omega)} \|u\|_{2,\Omega} \tag{3.5}$$

to be found in [1, Lemma 7.16]. Using Young's inequality, we finally obtain

$$\|u\|_{2,\partial\Omega}^2 \leq C \|u\|_{H^1(\Omega)} \|u\|_{2,\Omega} \leq \varepsilon \|u\|_{H^1(\Omega)}^2 + \frac{C}{\varepsilon} \|u\|_{2,\Omega}^2$$
$$\leq \varepsilon \|\nabla u\|_{2,\Omega}^2 + \frac{C}{\varepsilon} \|u\|_{2,\Omega}^2, \tag{3.6}$$

where the last inequality follows from $\varepsilon < 1$. ∎

Remark. It should be pointed out that Lemma 1 holds for general smooth geometries. In our case, the boundary Γ represents the rescaled surface of a spherical droplet. Moreover, Lemma 1 will only be applied to functions $u \in H^1(\Omega)$ satisfying $u = 0$ on Γ_∞. Under these additional constraints, one obtains interpolation inequality (3.3) also directly from the divergence theorem

$$\|u\|_{2,\Gamma}^2 = -\int_\Omega \nabla \cdot (u^2 x) \, dx = -\int_\Omega 2u\nabla u \cdot x + 3u^2 \, dx$$
$$\leq 2C \int_\Omega |u||\nabla u| \, dx \leq \varepsilon \|\nabla u\|_{2,\Omega}^2 + \frac{C}{\varepsilon} \|u\|_{2,\Omega}^2, \tag{3.7}$$

taking into account $x \cdot n = -1$ for all $x \in \Gamma$ and $|x| \leq C$ for all $x \in \Omega$.

3.2. Well-posedness for given droplet radius

In this section, we apply the method of upper and lower solutions to show that the decoupled droplet evaporation problem given by (P3)–(P5) admits a unique weak solution if

$R \in \Sigma_{t_*}$ is given. The idea is to replace the original nonlinear boundary conditions at the droplet surface by the following linear ones [26]:

$$
\begin{aligned}
\frac{1}{R}\nabla T^k \cdot n + LT^k &= -J^{k-1} + LT^{k-1}, \\
\frac{1}{R}\nabla \rho^k \cdot n + \rho^k &= J^{k-1} + \rho^{k-1},
\end{aligned}
\tag{3.8}
$$

where L denotes the Lipschitz constant of ρ_{sat} and $J^{k-1} := J(T^{k-1}, \rho^{k-1})$ the explicit evaporation rate. By that, we obtain an iteration process $(T^{k-1}, \rho^{k-1}) \mapsto (T^k, \rho^k)$ converging to the desired weak solution.

Lemma 2. *Let $T^{k-1}, \rho^{k-1} \in L^2(I, H^1(\Omega))$ and $R \in \Sigma_{t_*}$ be given. Further assume that R is bounded away from zero in the sense that $R(t) \geq \eta > 0$ for almost every $t \in I$. Then, there exist unique weak solutions*

$$
T^k, \rho^k \in L^2(I, H^1(\Omega)) \quad \text{with} \quad \partial_t T^k, \partial_t \rho^k \in L^2(I, X^*)
\tag{3.9}
$$

of the linear iteration process governed by the weak formulations

$$
\begin{aligned}
\langle \partial_t T^k, \varphi \rangle &+ \int_\Omega \frac{1}{R^2}\nabla T^k \cdot \nabla \varphi + \frac{1}{R}\nabla T^k \cdot (v - \dot{R}x)\varphi \, dx + \frac{1}{R}\int_\Gamma LT^k \varphi \, d\sigma \\
&= \frac{1}{R}\int_\Gamma (LT^{k-1} - J^{k-1})\varphi \, d\sigma,
\end{aligned}
\tag{3.10}
$$

$$
\begin{aligned}
\langle \partial_t \rho^k, \varphi \rangle &+ \int_\Omega \frac{1}{R^2}\nabla \rho^k \cdot \nabla \varphi + \frac{1}{R}\nabla \rho^k \cdot (v - \dot{R}x)\varphi \, dx + \frac{1}{R}\int_\Gamma \rho^k \varphi \, d\sigma \\
&= \frac{1}{R}\int_\Gamma (\rho^{k-1} + J^{k-1})\varphi \, d\sigma
\end{aligned}
\tag{3.11}
$$

for all test functions $\varphi \in X$ such that the initial and drying conditions

$$
T^k(0) = T_0 \quad \text{and} \quad \rho^k(0) = \rho_0 \quad \text{in } \Omega,
\tag{3.12}
$$

$$
T^k = T_\infty \quad \text{and} \quad \rho^k = \rho_\infty \quad \text{on } \Gamma_\infty
\tag{3.13}
$$

are fulfilled. Moreover, the weak solutions satisfy the following energy estimates:

$$
\begin{aligned}
\sup_{t \in I} \|T^k - T_\infty\|_{2,\Omega}^2 &+ \|\nabla T^k\|_{2,I \times \Omega}^2 \leq C[\|T_0 - T_\infty\|_{2,\Omega}^2 \\
&+ \|L(T^{k-1} - T_\infty) - J^{k-1}\|_{2,I \times \Gamma}^2],
\end{aligned}
\tag{3.14}
$$

$$
\begin{aligned}
\sup_{t \in I} \|\rho^k - \rho_\infty\|_{2,\Omega}^2 &+ \|\nabla \rho^k\|_{2,I \times \Omega}^2 \leq C[\|\rho_0 - \rho_\infty\|_{2,\Omega}^2 \\
&+ \|\rho^{k-1} - \rho_\infty + J^{k-1}\|_{2,I \times \Gamma}^2],
\end{aligned}
\tag{3.15}
$$

$$
\|\partial_t T^k\|_{L^2(I, X^*)}^2 \leq C[\|T_0 - T_\infty\|_{2,\Omega}^2 + \|L(T^{k-1} - T_\infty) - J^{k-1}\|_{2,I \times \Gamma}^2],
\tag{3.16}
$$

$$\|\partial_t \rho^k\|^2_{L^2(I,X^*)} \leq C[\|\rho_0 - \rho_\infty\|^2_{2,\Omega} + \|\rho^{k-1} - \rho_\infty + J^{k-1}\|^2_{2,I\times\Gamma}], \tag{3.17}$$

where the constant $C > 0$ depends on the positive lower bound η of the droplet radius.

Proof. The unique existence of the weak solutions T^k and ρ^k follows from Galerkin's method as carried out in [13,20] for similar linear parabolic problems. Testing (3.10) with $\varphi = T^k - T_\infty =: w^k$ implies

$$\frac{1}{2}\frac{d}{dt}\|w^k\|^2_{2,\Omega} + \frac{1}{R^2}\|\nabla w^k\|^2_{2,\Omega} - \frac{\dot{R}}{R}\int_\Omega (\nabla w^k \cdot x)w^k \, dx + \frac{L}{R}\|w^k\|^2_{2,\Gamma}$$
$$= \frac{1}{R}\int_\Gamma (Lw^{k-1} - J^{k-1})w^k \, d\sigma, \tag{3.18}$$

since v is divergence free and tangential at the droplet surface. Applying Hölder's inequality yields

$$\frac{1}{2}\frac{d}{dt}\|w^k\|^2_{2,\Omega} + \|\nabla w^k\|^2_{2,\Omega}$$
$$\leq C[\|\nabla w^k\|_{2,\Omega}\|w^k\|_{2,\Omega} + \|Lw^{k-1} - J^{k-1}\|_{2,\Gamma}\|w^k\|_{2,\Gamma}], \tag{3.19}$$

due to $|\dot{R}| \leq J_\infty$ and R being bounded away from zero. The estimate

$$\frac{1}{2}\frac{d}{dt}\|w^k\|^2_{2,\Omega} + \|\nabla w^k\|^2_{2,\Omega}$$
$$\leq C\left[\varepsilon\|\nabla w^k\|^2_{2,\Omega} + \frac{1}{\varepsilon}\|w^k\|^2_{2,\Omega} + \|Lw^{k-1} - J^{k-1}\|^2_{2,\Gamma}\right] \tag{3.20}$$

then follows from Young's inequality with $\varepsilon > 0$ and the interpolation inequality from Lemma 1. The choice $\varepsilon = 1/(2C)$ allows us to absorb the L^2-norm of the gradient. Applying Grönwall's lemma to the resulting inequality gives us

$$\frac{d}{dt}\|w^k\|^2_{2,\Omega} + \|\nabla w^k\|^2_{2,\Omega} \leq C[\|w^k\|^2_{2,\Omega} + \|Lw^{k-1} - J^{k-1}\|^2_{2,\Gamma}] \tag{3.21}$$

and implies (3.14), while (3.15) can be derived analogously. On the other hand, we obtain

$$|\langle\partial_t T^k, \varphi\rangle| \leq C[\|\nabla w^k\|_{2,\Omega} + \|Lw^{k-1} - J^{k-1}\|_{2,\Gamma}]\|\varphi\|_X \tag{3.22}$$

directly from (3.10) by applying Hölder's inequality, since (A6) implies $v \in L^\infty(\Omega)$. The estimate

$$\|\partial_t T^k\|_{X^*} \leq C[\|\nabla w^k\|_{2,\Omega} + \|Lw^{k-1} - J^{k-1}\|_{2,\Gamma}] \tag{3.23}$$

then follows from the fact that (3.22) holds for all $\varphi \in X$. Inserting (3.14) into the resulting inequality

$$\|\partial_t T^k\|^2_{L^2(I,X^*)} \leq C[\|\nabla w^k\|^2_{2,I\times\Omega} + \|Lw^{k-1} - J^{k-1}\|^2_{2,I\times\Gamma}] \tag{3.24}$$

finally implies (3.16), while (3.17) can be derived analogously. ∎

We are now in the position to show the well-posedness of (P3)–(P5) for given droplet radius. Recall from assumption (A5) that the drying conditions are required to satisfy $\rho_{\text{sat}}(T_\infty) \geq \rho_\infty$ such that the droplet actually evaporates. In the following proof, the constant tuples (T_*, ρ_∞) and (T_∞, ρ_*) will serve as lower and upper bounds for the weak solution (T, ρ) of the decoupled droplet evaporation problem:

Proposition 1. *Assume $R \in \Sigma_{t_*}$ to be given and bounded away from zero. Further suppose that the initial values $T_0, \rho_0 \in L^2(\Omega)$ are bounded by the drying conditions and constants from* (A5) *as follows:*

$$T_* \leq T_0(x) \leq T_\infty \quad and \quad \rho_\infty \leq \rho_0(x) \leq \rho_* \tag{3.25}$$

for almost every $x \in \Omega$. Then, the decoupled droplet evaporation problem (see (P3)–(P5)*) admits a unique weak solution*

$$(T, \rho) \in L^2(I, H^1(\Omega))^2 \quad with \quad (\partial_t T, \partial_t \rho) \in L^2(I, X^*)^2 \tag{3.26}$$

satisfying the pointwise lower and upper bounds

$$T_* \leq T(t, x) \leq T_\infty \quad and \quad \rho_\infty \leq \rho(t, x) \leq \rho_* \tag{3.27}$$

for almost every $(t, x) \in I \times \Omega$.

Proof. Following [13, 26], we apply the method of upper and lower solutions. Therefore, let us consider the iteration process $(T^{k-1}, \rho^{k-1}) \mapsto (T^k, \rho^k)$ defined by the linear parabolic problems from Lemma 2.

Step 1. We show by induction that the iterative solutions resulting from $(T^0, \rho^0) = (T_\infty, \rho_*)$ satisfy

$$T_* \leq T^k \leq T^{k-1} \leq T_\infty \quad and \quad \rho_\infty \leq \rho^k \leq \rho^{k-1} \leq \rho_* \tag{3.28}$$

for all $k \in \mathbb{N}$. Let us verify $T_* \leq T^1 \leq T_\infty$ first. Using

$$w := (T^1 - T_\infty)^+ = \begin{cases} T^1 - T_\infty & \text{if } T^1 > T_\infty, \\ 0 & \text{if } T^1 \leq T_\infty \end{cases} \tag{3.29}$$

as a test function in (3.10) yields the identity

$$\frac{1}{2}\frac{d}{dt}\|w\|_{2,\Omega}^2 + \frac{1}{R^2}\|\nabla w\|_{2,\Omega}^2 + \frac{L}{R}\|w\|_{2,\Gamma}^2 = \frac{\dot{R}}{R}\int_\Omega (\nabla w \cdot x)w \, dx, \tag{3.30}$$

taking into account $J^0 = 0$, $\nabla \cdot v = 0$ in Ω and $v \cdot n = 0$ on Γ. From Young's inequality we infer

$$\frac{\dot{R}}{R}\int_\Omega (\nabla w \cdot x)w \, dx \leq \varepsilon\|\nabla w\|_{2,\Omega}^2 + \frac{C}{\varepsilon}\|w\|_{2,\Omega}^2 \tag{3.31}$$

due to the term $|\dot{R}|/R$ and the domain Ω being bounded. Inserting (3.31) with $\varepsilon = 1/(2R^2)$ into (3.30) allows us to absorb the L^2-norm of the gradient. Applying Grönwall's lemma to the resulting inequality

$$\frac{d}{dt}\|w\|_{2,\Omega}^2 \le C\|w\|_{2,\Omega}^2 \tag{3.32}$$

implies $w = 0$, and thus $T^1 \le T_\infty$, taking into account that $w(0) = (T_0 - T_\infty)^+ = 0$. On the other hand, testing (3.10) with $\tilde{w} := (T_* - T^1)^+$ as defined above implies

$$\frac{1}{2}\frac{d}{dt}\|\tilde{w}\|_{2,\Omega}^2 + \frac{1}{R^2}\|\nabla\tilde{w}\|_{2,\Omega}^2 + \frac{L}{R}\|\tilde{w}\|_{2,\Gamma}^2 + \frac{L}{R}\int_\Gamma (T_\infty - T_*)\tilde{w}\,d\sigma$$
$$= \frac{\dot{R}}{R}\int_\Omega (\nabla\tilde{w}\cdot x)\tilde{w}\,dx, \tag{3.33}$$

which allows us to conclude $T_* \le T^1$ as before. It should be mentioned that $\tilde{w}$ is an admissible test function, since $T_* \le T_\infty$ guarantees $\tilde{w} = 0$ on Γ_∞. The inequalities $\rho_\infty \le \rho^1 \le \rho_*$ for the vapor mass density are obtained analogously.

Now let us assume that (3.28) already holds for some $k \in \mathbb{N}$. Subtracting the weak formulations for T^{k+1} and T^k after inserting $w^{k+1} := (T^{k+1} - T^k)^+$ as a test function leads to the identity

$$\frac{1}{2}\frac{d}{dt}\|w^{k+1}\|_{2,\Omega}^2 + \frac{1}{R^2}\|\nabla w^{k+1}\|_{2,\Omega}^2 + \frac{L}{R}\|w^{k+1}\|_{2,\Gamma}^2$$
$$= \frac{\dot{R}}{R}\int_\Omega (\nabla w^{k+1}\cdot x)w^{k+1}\,dx + \int_\Gamma [J^{k-1} - J^k - L(T^{k-1} - T^k)]w^{k+1}\,d\sigma \tag{3.34}$$

for all $k \ge 2$. Since our induction hypothesis (3.28) implies

$$J^{k-1} - J^k \le \rho_{\text{sat}}(T^{k-1}) - \rho_{\text{sat}}(T^k) \le L(T^{k-1} - T^k), \tag{3.35}$$

we obtain $w^{k+1} = 0$, and thus, $T^{k+1} \le T^k$ from the same Grönwall argument as before. Likewise, testing (3.10) with $\tilde{w}^{k+1} := (T_* - T^{k+1})^+$ yields $T_* \le T^{k+1}$, taking into account that

$$\rho_{\text{sat}}(T^k) - \rho^k \le \rho_{\text{sat}}(T^k) - \rho_\infty \le L(T^k - T_*) \tag{3.36}$$

already holds. The remaining inequalities $\rho_\infty \le \rho^{k+1} \le \rho^k$ for the vapor mass density are obtained analogously. This concludes the proof of (3.28) for all $k \in \mathbb{N}$ by induction.

Step 2. We are now in the position to show that the iteration process $\{(T^k, \rho^k)\}_{k\in\mathbb{N}}$ from Lemma 2 converges (up to a subsequence) to the desired weak solution (T, ρ) of the decoupled evaporation problem. From (3.28) we infer that the pointwise limits

$$T(t,x) := \lim_{k\to\infty} T^k(t,x) \quad \text{and} \quad \rho(t,x) := \lim_{k\to\infty} \rho^k(t,x) \tag{3.37}$$

exist for almost every $(t,x) \in I \times \Omega$. In fact, we have $T^k \to T$ and $\rho^k \to \rho$ in $L^2(I \times \Omega)$ and $L^2(I \times \Gamma)$ due to Lebesgue's dominated convergence theorem. According to the

energy estimates from Lemma 2, it follows from (3.28) that the iterative solutions $\{T^k\}_{k \in \mathbb{N}}$ and $\{\rho^k\}_{k \in \mathbb{N}}$ are both bounded in $L^2(I, H^1(\Omega))$. Likewise, their time derivatives $\{\partial_t T^k\}_{k \in \mathbb{N}}$ and $\{\partial_t \rho^k\}_{k \in \mathbb{N}}$ are both bounded in $L^2(I, X^*)$. Hence, there exists a subsequence $\{(T^{k_l}, \rho^{k_l})\}_{l \in \mathbb{N}}$ such that

$$
\begin{aligned}
T^{k_l} \rightharpoonup T \quad &\text{and} \quad \rho^{k_l} \rightharpoonup \rho \quad \text{weakly in } L^2(I, H^1(\Omega)), \\
\partial_t T^{k_l} \rightharpoonup \partial_t T \quad &\text{and} \quad \partial_t \rho^{k_l} \rightharpoonup \partial_t \rho \quad \text{weakly in } L^2(I, X^*).
\end{aligned}
\tag{3.38}
$$

Consequently, the respective limits T and ρ satisfy the following weak formulations:

$$
\langle \partial_t T, \varphi \rangle + \int_\Omega \frac{1}{R^2} \nabla T \cdot \nabla \varphi + \frac{1}{R} \nabla T \cdot (v - \dot{R}x) \varphi \, dx + \frac{1}{R} \int_\Gamma L T \varphi \, d\sigma
$$
$$
= \frac{1}{R} \int_\Gamma [LT - J(T, \rho)] \varphi \, d\sigma,
\tag{3.39}
$$
$$
\langle \partial_t \rho, \varphi \rangle + \int_\Omega \frac{1}{R^2} \nabla \rho \cdot \nabla \varphi + \frac{1}{R} \nabla \rho \cdot (v - \dot{R}x) \varphi \, dx + \frac{1}{R} \int_\Gamma \rho \varphi \, d\sigma
$$
$$
= \frac{1}{R} \int_\Gamma [\rho + J(T, \rho)] \varphi \, d\sigma
\tag{3.40}
$$

for almost every $t \in I$ and all test functions $\varphi \in X$. Notice that the convergence $J^{k_l} \to J(T, \rho)$ in $L^2(I \times \Gamma)$ follows from ρ_{sat} being Lipschitz continuous. Subtracting the redundant boundary integrals yields the desired weak formulation (see (P2) and (P3)) of the decoupled evaporation problem.

Step 3. To show uniqueness, let (T_1, ρ_1) and (T_2, ρ_2) be two weak solutions of the decoupled droplet evaporation problem given by (P3)–(P5). Then, their differences $\delta T := T_1 - T_2$ and $\delta \rho := \rho_1 - \rho_2$ satisfy

$$
\frac{1}{2} \frac{d}{dt} \|\delta T\|_{2,\Omega}^2 + \frac{1}{R^2} \|\nabla \delta T\|_{2,\Omega}^2
$$
$$
= \frac{\dot{R}}{R} \int_\Omega (\nabla \delta T \cdot x) \delta T \, dx - \frac{1}{R} \int_\Gamma (\delta \rho_{\text{sat}} - \delta \rho) \delta T \, d\sigma,
\tag{3.41}
$$
$$
\frac{1}{2} \frac{d}{dt} \|\delta \rho\|_{2,\Omega}^2 + \frac{1}{R^2} \|\nabla \delta \rho\|_{2,\Omega}^2
$$
$$
= \frac{\dot{R}}{R} \int_\Omega (\nabla \delta \rho \cdot x) \delta \rho \, dx + \frac{1}{R} \int_\Gamma (\delta \rho_{\text{sat}} - \delta \rho) \delta \rho \, d\sigma
\tag{3.42}
$$

with $\delta \rho_{\text{sat}} := \rho_{\text{sat}}(T_1) - \rho_{\text{sat}}(T_2)$. Applying Young's inequality with $\varepsilon > 0$ yields

$$
\frac{\dot{R}}{R} \int_\Omega (\nabla \delta T \cdot x) \delta T \, dx \le \varepsilon \|\nabla \delta T\|_{2,\Omega}^2 + \frac{C}{\varepsilon} \|\delta T\|_{2,\Omega}^2,
\tag{3.43}
$$
$$
\frac{\dot{R}}{R} \int_\Omega (\nabla \delta \rho \cdot x) \delta \rho \, dx \le \varepsilon \|\nabla \delta \rho\|_{2,\Omega}^2 + \frac{C}{\varepsilon} \|\delta \rho\|_{2,\Omega}^2,
\tag{3.44}
$$

which allows us to absorb the L^2-norms of the gradients. Therefore, adding (3.41) and (3.42) implies

$$
\frac{d}{dt}(\|\delta T\|_{2,\Omega}^2 + \|\delta\rho\|_{2,\Omega}^2) + \|\nabla\delta T\|_{2,\Omega}^2 + \|\nabla\delta\rho\|_{2,\Omega}^2
$$
$$
\leq C(\|\delta T\|_{2,\Omega}^2 + \|\delta\rho\|_{2,\Omega}^2) - \frac{1}{R}\int_\Gamma (\delta\rho_{\mathrm{sat}} - \delta\rho)(\delta T - \delta\rho)\,d\sigma, \qquad (3.45)
$$

since R is bounded away from zero. Taking into account that ρ_{sat} is Lipschitz continuous, we obtain

$$
-\frac{1}{R}\int_\Gamma (\delta\rho_{\mathrm{sat}} - \delta\rho)(\delta T - \delta\rho)\,d\sigma \leq C(\|\delta T\|_{2,\Gamma}^2 + \|\delta\rho\|_{2,\Gamma}^2)
$$
$$
\leq \varepsilon(\|\nabla\delta T\|_{2,\Omega}^2 + \|\nabla\delta\rho\|_{2,\Omega}^2) + \frac{C}{\varepsilon}(\|\delta T\|_{2,\Omega}^2 + \|\delta\rho\|_{2,\Omega}^2), \qquad (3.46)
$$

using the interpolation inequality from Lemma 1. Inserting (3.46) with $\varepsilon = 1/2$ into (3.45) allows us to absorb the L^2-norms of the gradients. Applying Grönwall's lemma to the resulting inequality

$$
\frac{d}{dt}(\|\delta T\|_{2,\Omega}^2 + \|\delta\rho\|_{2,\Omega}^2) \leq C(\|\delta T\|_{2,\Omega}^2 + \|\delta\rho\|_{2,\Omega}^2) \qquad (3.47)
$$

finally implies $\|\delta T(t)\|_{2,\Omega}^2 + \|\delta\rho(t)\|_{2,\Omega}^2 = 0$ for all $t \in I$, and thus, $T_1 = T_2$ and $\rho_1 = \rho_2$ almost everywhere in $I \times \Omega$. ∎

3.3. Short time existence for the coupled evaporation problem

We are now in the position to show that the coupled droplet evaporation problem from Section 2 admits a unique weak solution in the sense of Definition 1 if the time interval $I = [0, t_*)$ is sufficiently small. From now on, the droplet radius R is no longer given but considered as an additional unknown. First of all, we need to understand how the weak solution of the decoupled problem from Proposition 1 depends on the corresponding droplet radius.

Proposition 2. *Let $T_{0,1}, \rho_{0,1} \in L^2(\Omega)$ and $T_{0,2}, \rho_{0,2} \in L^2(\Omega)$ be two pairs of initial values, both bounded by (3.25) almost everywhere in Ω. Further assume that the droplet radii $R_1, R_2 \in \Sigma_{t_*}$ are bounded away from zero in the sense that $R_1(t) \geq \eta_1 > 0$ and $R_2(t) \geq \eta_2 > 0$ for almost every $t \in I$. Then, the corresponding weak solutions (T_1, ρ_1) and (T_2, ρ_2) of the decoupled droplet evaporation problem (P3)–(P5) satisfy the following stability estimates:*

$$
\sup_{t \in I} \|T_1 - T_2\|_{2,\Omega}^2 + \|\nabla(T_1 - T_2)\|_{2,I\times\Omega}^2
$$
$$
\leq C(\|T_{0,1} - T_{0,2}\|_{2,\Omega}^2 + \|\rho_{0,1} - \rho_{0,2}\|_{2,\Omega}^2 + \|R_1 - R_2\|_{H^1(I)}^2), \qquad (3.48)
$$

$$\sup_{t \in I} \| \rho_1 - \rho_2 \|_{2,\Omega}^2 + \| \nabla (\rho_1 - \rho_2) \|_{2, I \times \Omega}^2$$

$$\leq C (\| T_{0,1} - T_{0,2} \|_{2,\Omega}^2 + \| \rho_{0,1} - \rho_{0,2} \|_{2,\Omega}^2 + \| R_1 - R_2 \|_{H^1(I)}^2), \qquad (3.49)$$

where the Lipschitz constant $C > 0$ depends on the lower bound $\eta := \min\{\eta_1, \eta_2\}$ of both droplet radii.

Proof. Let us first briefly outline the main idea of our proof: after subtracting the weak formulations of both solutions, we sort all defect terms to the right-hand side and estimate them with respect to the difference of both droplet radii. Applying Grönwall's lemma to the resulting inequality then finally implies the desired stability estimate.

Since $R_1, R_2 \in \Sigma_{t_*}$ are bounded away from zero, the corresponding weak solutions (T_1, ρ_1) and (T_2, ρ_2) from Proposition 1 are well-defined. Testing (P3) with the difference $\varphi = T_1 - T_2 =: \delta T$ yields two equations for T_1 and T_2, respectively. Subtracting one from the other implies

$$\langle \partial_t \delta T, \delta T \rangle + \int_\Omega \nabla \left(\frac{T_1}{R_1^2} - \frac{T_2}{R_2^2} \right) \cdot \nabla \delta T \, dx + \int_\Omega \nabla \cdot \left(\frac{T_1 v_1}{R_1} - \frac{T_2 v_2}{R_2} \right) \delta T \, dx$$

$$- \int_\Omega \nabla \left(\frac{\dot{R}_1 T_1}{R_1} - \frac{\dot{R}_2 T_2}{R_2} \right) \cdot x \delta T \, dx + \int_\Gamma \left(\frac{J_1}{R_1} - \frac{J_2}{R_2} \right) \delta T \, d\sigma = 0 \qquad (3.50)$$

with the evaporation rates $J_i := J(T_i, \rho_i)$ for $i \in \{1, 2\}$. We define $\delta R := R_1 - R_2$, $\delta \dot{R} := \dot{R}_1 - \dot{R}_2$, $\delta v := v_1 - v_2$, and $\delta J := J_1 - J_2$ for the ease of presentation. Inserting the decompositions

$$\frac{T_1}{R_1^2} - \frac{T_2}{R_2^2} = \frac{\delta T}{R_1^2} - \delta R \frac{R_1 + R_2}{R_1 R_2} T_2, \qquad (3.51)$$

$$\frac{T_1 v_1}{R_1} - \frac{T_2 v_2}{R_2} = \frac{\delta T v_1}{R_1} + \left(\frac{\delta v}{R_1} - \frac{\delta R v_2}{R_1 R_2} \right) T_2, \qquad (3.52)$$

$$\frac{\dot{R}_1 T_1}{R_1} - \frac{\dot{R}_2 T_2}{R_2} = \frac{\dot{R}_1}{R_1} \delta T + \left(\frac{\delta \dot{R}}{R_1} - \frac{\delta R \dot{R}_2}{R_1 R_2} \right) T_2, \qquad (3.53)$$

$$\frac{J_1}{R_1} - \frac{J_2}{R_2} = \frac{\delta J}{R_1} - \frac{\delta R J_2}{R_1 R_2} \qquad (3.54)$$

into (3.50) and sorting the resulting terms yields

$$\frac{1}{2} \frac{d}{dt} \| \delta T \|_{2,\Omega}^2 + \frac{1}{R_1^2} \| \nabla \delta T \|_{2,\Omega}^2$$

$$= \frac{\dot{R}_1}{R_1} \int_\Omega (\nabla \delta T \cdot x) \delta T \, dx - \frac{1}{R_1} \int_\Gamma \delta J \delta T \, d\sigma + d_T, \qquad (3.55)$$

where the temperature defect

$$d_T := \frac{1}{R_1 R_2} \int_\Omega \nabla T_2 \cdot (\delta R v_2 - R_2 \delta v + \delta \dot{R} R_2 x - \delta R \dot{R}_2 x) \delta T \, dx + \frac{\delta R}{R_1 R_2} \int_\Gamma J_2 \delta T \, d\sigma$$

$$+ \delta R \frac{R_1 + R_2}{R_1 R_2} \int_\Omega \nabla T_2 \cdot \nabla \delta T \, dx \qquad (3.56)$$

contains all products with δR, $\delta \dot{R}$, or δv. Notice that the integral of $(\nabla \delta T \cdot v_1) \delta T$ over Ω vanishes, since v_1 is divergence free and tangential at the droplet surface. Young's inequality implies

$$\frac{\dot{R}_1}{R_1} \int_\Omega (\nabla \delta T \cdot x) \delta T \, dx \leq \frac{1}{2R_1^2} \|\nabla \delta T\|_{2,\Omega}^2 + C \|\delta T\|_{2,\Omega}^2, \tag{3.57}$$

taking into account $|\dot{R}_1| \leq J_\infty$ and $|\nabla \delta T \cdot x| \leq C |\nabla \delta T|$, due to Ω being bounded. Inserting (3.57) into (3.55) allows us to absorb the L^2-norm of the gradient. By that, we obtain

$$\frac{d}{dt} \|\delta T\|_{2,\Omega}^2 + \frac{1}{R_1^2} \|\nabla \delta T\|_{2,\Omega}^2 \leq C \|\delta T\|_{2,\Omega}^2 - \frac{2}{R_1} \int_\Gamma \delta J \delta T \, d\sigma + 2d_T \tag{3.58}$$

for almost every $t \in I$.

Likewise, testing (P2) with $\varphi = \rho_1 - \rho_2 =: \delta\rho$ yields

$$\frac{d}{dt} \|\delta\rho\|_{2,\Omega}^2 + \frac{1}{R_1^2} \|\nabla \delta\rho\|_{2,\Omega}^2 \leq C \|\delta\rho\|_{2,\Omega}^2 + \frac{2}{R_1} \int_\Gamma \delta J \delta\rho \, d\sigma + 2d_\rho \tag{3.59}$$

with the vapor mass defect d_ρ being defined by

$$d_\rho := \frac{1}{R_1 R_2} \int_\Omega \nabla \rho_2 \cdot \left(\delta R v_2 - R_2 \delta v + \delta \dot{R} R_2 x - \delta R \dot{R}_2 x \right) \delta\rho \, dx - \frac{\delta R}{R_1 R_2} \int_\Gamma J_2 \delta\rho \, d\sigma$$
$$+ \delta R \frac{R_1 + R_2}{R_1 R_2} \int_\Omega \nabla \rho_2 \cdot \nabla \delta\rho \, dx, \tag{3.60}$$

applying the same decompositions (see (3.51)–(3.54)) as before. Adding (3.58) and (3.59) implies

$$\frac{d}{dt} (\|\delta T\|_{2,\Omega}^2 + \|\delta\rho\|_{2,\Omega}^2) + \frac{1}{R_1^2} (\|\nabla \delta T\|_{2,\Omega}^2 + \|\nabla \delta\rho\|_{2,\Omega}^2)$$
$$\leq C(\|\delta T\|_{2,\Omega}^2 + \|\delta\rho\|_{2,\Omega}^2) + \frac{2}{R_1} \int_\Gamma |\delta J| |\delta T - \delta\rho| \, d\sigma + d, \tag{3.61}$$

where $d := 2(d_T + d_\rho)$ denotes the total defect. The rough estimate

$$2 \int_\Gamma |\delta J| |\delta T - \delta\rho| \, d\sigma \leq C(\|\delta T\|_{2,\Gamma}^2 + \|\delta\rho\|_{2,\Gamma}^2) \tag{3.62}$$

follows from ρ_{sat} being Lipschitz continuous. Together with interpolation inequality (3.3), we obtain

$$\frac{2}{R_1} \int_\Gamma |\delta J| |\delta T - \delta\rho| \, d\sigma$$
$$\leq \frac{1}{2R_1^2} (\|\nabla \delta T\|_{2,\Omega}^2 + \|\nabla \delta\rho\|_{2,\Omega}^2) + C(\|\delta T\|_{2,\Omega}^2 + \|\delta\rho\|_{2,\Omega}^2), \tag{3.63}$$

which allows us to absorb the L^2-norms of the gradients. Therefore, inserting (3.63) into (3.61) implies

$$\frac{d}{dt}(\|\delta T\|_{2,\Omega}^2 + \|\delta\rho\|_{2,\Omega}^2) + \frac{1}{2R_1^2}(\|\nabla\delta T\|_{2,\Omega}^2 + \|\nabla\delta\rho\|_{2,\Omega}^2)$$
$$\leq C(\|\delta T\|_{2,\Omega}^2 + \|\delta\rho\|_{2,\Omega}^2) + d \tag{3.64}$$

for almost every $t \in I$. As carried out in the appendix, the total defect is bounded by

$$|d| \leq \frac{1}{4R_1^2}(\|\nabla\delta T\|_{2,\Omega}^2 + \|\nabla\delta\rho\|_{2,\Omega}^2) + C[\|\delta T\|_{2,\Omega}^2 + \|\delta\rho\|_{2,\Omega}^2$$
$$+ (1 + \|\nabla T_2\|_{2,\Omega}^2 + \|\nabla\rho_2\|_{2,\Omega}^2)\delta R^2 + \delta\dot{R}^2], \tag{3.65}$$

which directly follows from the repeated application of Hölder's and Young's inequalities together with the interpolation inequality from Lemma 1. After combining (3.64) and (3.65), we absorb the L^2-norms of the gradients. By that, we obtain

$$\frac{d}{dt}(\|\delta T\|_{2,\Omega}^2 + \|\delta\rho\|_{2,\Omega}^2) + \|\nabla\delta T\|_{2,\Omega}^2 + \|\nabla\delta\rho\|_{2,\Omega}^2$$
$$\leq C[\|\delta T\|_{2,\Omega}^2 + \|\delta\rho\|_{2,\Omega}^2 + (1 + \|\nabla T_2\|_{2,\Omega}^2 + \|\nabla\rho_2\|_{2,\Omega}^2)\delta R^2 + \delta\dot{R}^2], \tag{3.66}$$

since $R_1 \geq \eta_1$ is bounded away from zero. Integration over time implies

$$E(t) \leq E(0) + C\int_0^t E(\tau)\,d\tau + D(t) \tag{3.67}$$

with the energy

$$E(t) := \|\delta T(t)\|_{2,\Omega}^2 + \|\delta\rho(t)\|_{2,\Omega}^2 + \int_0^t \|\nabla\delta T\|_{2,\Omega}^2 + \|\nabla\delta\rho\|_{2,\Omega}^2\,d\tau \tag{3.68}$$

and the integrated total defect

$$D(t) := C\int_0^t \left(1 + \|\nabla T_2\|_{2,\Omega}^2 + \|\nabla\rho_2\|_{2,\Omega}^2\right)\delta R^2 + \delta\dot{R}^2\,d\tau \tag{3.69}$$

for $t \in I$. We are now in the position to apply Grönwall's lemma. The latter implies

$$E(t) \leq \exp(Ct)(D(t) + E(0)), \tag{3.70}$$

since D is nondecreasing. From the Sobolev embedding theorem in one dimension, we know that $|\delta R|^2 \leq C\|\delta R\|_{H^1(I)}^2$. Inserting this into (3.69) yields the desired upper bound

$$D(t) \leq C[1 + t + \|\nabla T_2\|_{2,I\times\Omega}^2 + \|\nabla\rho_2\|_{2,I\times\Omega}^2]\|\delta R\|_{H^1(I)}^2 \leq C\|\delta R\|_{H^1(I)}^2 \tag{3.71}$$

for the integrated total defect. Therefore, combining inequalities (3.70) and (3.71) concludes our proof. ∎

Recall from the beginning of this section that finding a weak solution in the sense of Definition 1 can be reformulated as a fixed-point problem. In the following, we finally apply Banach's fixed-point theorem to prove the short time existence of a unique weak solution to our droplet evaporation problem:

Theorem 1. *Let the initial values $T_0, \rho_0 \in L^2(\Omega)$ be bounded by* (3.25) *almost everywhere in Ω. Then, the Volterra operator $\mathcal{T} : \Sigma_{t_*} \to \Sigma_{t_*}$ defined by* (3.1) *is a contraction with respect to the H^1-norm if the underlying time interval $I = [0, t_*)$ is sufficiently small. Consequently, the droplet evaporation problem from Section 2 admits a unique weak solution (R, T, ρ) on I in the sense of Definition 1.*

Proof. Assume $t_* < R_0/(2J_\infty)$ such that the droplet radii in Σ_{t_*} are uniformly bounded away from zero. Now let $R_1, R_2 \in \Sigma_{t_*}$ and define $\delta\mathcal{T} := \mathcal{T}(R_1) - \mathcal{T}(R_2)$. From $\delta\mathcal{T}(0) = 0$, we infer

$$\|\delta\mathcal{T}\|_{H^1(I)}^2 = \|\delta\mathcal{T}\|_{2,I}^2 + \|\delta\dot{\mathcal{T}}\|_{2,I}^2 \le \Big(1 + \int_I t \, dt\Big)\|\delta\dot{\mathcal{T}}\|_{2,I}^2 = \Big(1 + \frac{t_*^2}{2}\Big)\|\delta\dot{\mathcal{T}}\|_{2,I}^2, \tag{3.72}$$

taking into account $|\delta\mathcal{T}(t)| \le \sqrt{t}\|\delta\dot{\mathcal{T}}\|_{2,I}$ due to Hölder's inequality. The latter further implies

$$\|\delta\dot{\mathcal{T}}\|_{2,I}^2 = \int_I \Big(\frac{1}{4\pi}\int_\Gamma \delta J \, d\sigma\Big)^2 d\tau \le \frac{1}{4\pi}\int_I \int_\Gamma \delta J^2 \, d\sigma \, d\tau, \tag{3.73}$$

since $|\Gamma| = 4\pi$. Recall that the rough estimate $\delta J^2 \le C(\delta T^2 + \delta\rho^2)$ follows from Young's inequality and ρ_{sat} being Lipschitz continuous. Together with Lemma 1, we thus obtain

$$\|\delta\dot{\mathcal{T}}\|_{2,I}^2 \le C \int_I \varepsilon(\|\nabla\delta T\|_{2,\Omega}^2 + \|\nabla\delta\rho\|_{2,\Omega}^2) + \frac{1}{\varepsilon}(\|\delta T\|_{2,\Omega}^2 + \|\delta\rho\|_{2,\Omega}^2)\, d\tau$$

$$\le C\Big[\varepsilon(\|\nabla\delta T\|_{2,I\times\Omega}^2 + \|\nabla\delta\rho\|_{2,I\times\Omega}^2) + \frac{t_*}{\varepsilon}\sup_{t\in I}(\|\delta T\|_{2,\Omega}^2 + \|\delta\rho\|_{2,\Omega}^2)\Big], \quad (3.74)$$

which finally makes Proposition 2 applicable. By that, we arrive at the desired inequality

$$\|\delta\mathcal{T}\|_{H^1(I)}^2 \le C\Big(\varepsilon + \frac{t_*}{\varepsilon}\Big)\|\delta R\|_{H^1(I)}^2 \tag{3.75}$$

whose Lipschitz constant becomes strictly smaller than one if ε and t_* are chosen accordingly. For instance, $\varepsilon = 1/(2C)$ and $t_* < 1/(2C)^2$ would be one possible choice. Hence, the operator $\mathcal{T}$ turns out to be a contraction on Σ_{t_*} if $t_* > 0$ is sufficiently small. The short time existence of a unique weak solution (R, T, ρ) then follows from Banach's fixed-point theorem. ∎

We will now show stability of solutions with respect to perturbed initial values.

Theorem 2. *Assume that (T_1, ρ_1, R_1) and (T_2, ρ_2, R_2) are two solutions for initial values $(T_{0,1}, \rho_{0,1}, R_{0,1})$ and $(T_{0,2}, \rho_{0,2}, R_{0,2})$ on a common time interval $I = (0, t_*)$. Then, we*

have

$$
\sup_{t \in I}(\|T_1 - T_2\|_{2,\Omega}^2 + \|\rho_1 - \rho_2\|_{2,\Omega}^2 + |R_1 - R_2|^2) + \|\nabla(T_1 - T_2)\|_{2,I \times \Omega}^2
$$

$$
+ \|\nabla(\rho_1 - \rho_2)\|_{2,I \times \Omega}^2 \leq C_{T_2,\rho_2}(\|T_{0,1} - T_{0,2}\|_{2,\Omega}^2 + \|\rho_{0,1} - \rho_{0,2}\|_{2,\Omega}^2 + |R_{0,1} - R_{0,2}|^2) \tag{3.76}
$$

with a constant C_{T_2,ρ_2} *depending on* $\|\nabla T_2\|_{2,I \times \Omega}^2 + \|\nabla \rho_2\|_{2,I \times \Omega}^2$ *and* t_*.

Proof. Since all arguments of Proposition 2 apply, in particular, if (T_1, ρ_1, R_1) and (T_2, ρ_2, R_2) solve the coupled problem, we first proceed as in the proof of Proposition 2 to obtain (3.66). Adding

$$
\frac{d}{dt}|\delta R|^2 = 2\delta R \delta \dot{R} \leq |\delta R|^2 + |\delta \dot{R}|^2 \tag{3.77}
$$

to (3.66) gives

$$
\frac{d}{dt}(\|\delta T\|_{2,\Omega}^2 + \|\delta \rho\|_{2,\Omega}^2 + |\delta R|^2) + \|\nabla \delta T\|_{2,\Omega}^2 + \|\nabla \delta \rho\|_{2,\Omega}^2
$$

$$
\leq (C+1)[\|\delta T\|_{2,\Omega}^2 + \|\delta \rho\|_{2,\Omega}^2 + (2 + \|\nabla T_2\|_{2,\Omega}^2 + \|\nabla \rho_2\|_{2,\Omega}^2)|\delta R|^2
$$

$$
+ |\delta \dot{R}|^2]. \tag{3.78}
$$

Since R_1 and R_2 satisfy the differential equation, we can use the arguments from the proof of Theorem 1 to derive the bound

$$
|\delta \dot{R}|^2 \leq C\varepsilon(\|\nabla \delta T\|_{2,\Omega}^2 + \|\nabla \delta \rho\|_{2,\Omega}^2) + \frac{C}{\varepsilon}(\|\delta T\|_{2,\Omega}^2 + \|\delta \rho\|_{2,\Omega}^2). \tag{3.79}
$$

Inserting this into (3.78) with a sufficiently small $\varepsilon > 0$ gives

$$
\frac{d}{dt}(\|\delta T\|_{2,\Omega}^2 + \|\delta \rho\|_{2,\Omega}^2 + |\delta R|^2) + \frac{1}{2}(\|\nabla \delta T\|_{2,\Omega}^2 + \|\nabla \delta \rho\|_{2,\Omega}^2)
$$

$$
\leq C[\|\delta T\|_{2,\Omega}^2 + \|\delta \rho\|_{2,\Omega}^2 + (2 + \|\nabla T_2\|_{2,\Omega}^2 + \|\nabla \rho_2\|_{2,\Omega}^2)|\delta R|^2]
$$

$$
\leq C(2 + \|\nabla T_2\|_{2,\Omega}^2 + \|\nabla \rho_2\|_{2,\Omega}^2)(\|\delta T\|_{2,\Omega}^2 + \|\delta \rho\|_{2,\Omega}^2 + |\delta R|^2). \tag{3.80}
$$

Integrating this over time, we obtain

$$
E(t) \leq E(0) + \int_0^t \beta(s)E(s)\,ds \tag{3.81}
$$

with the energy $E(t)$ and $\beta(s)$ given by

$$
E(t) := \|\delta T(t)\|_{2,\Omega}^2 + \|\delta \rho(t)\|_{2,\Omega}^2 + |\delta R(t)|^2
$$

$$
+ \int_0^t \|\nabla \delta T\|_{2,\Omega}^2 + \|\nabla \delta \rho\|_{2,\Omega}^2 \, d\tau, \tag{3.82}
$$

$$
\beta(s) := C(2 + \|\nabla T_2(s)\|_{2,\Omega}^2 + \|\nabla \rho_2(s)\|_{2,\Omega}^2). \tag{3.83}
$$

Notice that E is continuous, while $\beta \in L^1(0, t)$ is such that Grönwall's lemma [37, Lemma 29.2] yields

$$E(t) \leq E(0) + E(0) \int_0^t \beta(s) \exp\left(\int_0^s \beta(\tau)d\tau\right)ds$$
$$\leq E(0)(1 + \|\beta\|_{L^1(I)} \exp(\|\beta\|_{L^1(I)})). \tag{3.84}$$

This proves the assertion. ∎

3.4. Maximal time interval of existence

The weak solution (R, T, ρ) of the coupled evaporation problem is said to be maximal if it cannot be extended on a larger time interval. The following theorem shows that the maximal time interval can only be finite if the droplet evaporates completely:

Theorem 3. *Let the initial values $T_0, \rho_0 \in L^2(\Omega)$ be bounded by* (3.25) *almost every-where in Ω. Then, the droplet evaporation problem admits a unique weak solution (R, T, ρ) in the sense of Definition* 1 *whose time interval $I_{max} := [0, t_{max})$ is maximal. If $t_{max} < \infty$, then the droplet evaporates completely, meaning that*

$$\lim_{t \to t_{max}^-} R(t) = 0 \tag{3.85}$$

where $t \to t_{max}^-$ denotes the one-sided limit from below.

Proof. First of all, it should be mentioned that (3.85) is well defined, since the Sobolev embedding $H^1(I_{max}) \hookrightarrow C^0([0, t_{max}])$ ensures the required continuity of the droplet radius. Now assume that

$$R_{max} := \lim_{t \to t_{max}^-} R(t) > 0 \tag{3.86}$$

is strictly positive. According to the Lions–Magenes lemma, there exist $T_{max}, \rho_{max} \in L^2(\Omega)$ such that

$$\lim_{t \to t_{max}^-} \|T(t) - T_{max}\|_{2,\Omega} = 0 \quad \text{and} \quad \lim_{t \to t_{max}^-} \|\rho(t) - \rho_{max}\|_{2,\Omega} = 0. \tag{3.87}$$

According to Proposition 1, we have $\rho_\infty \leq \rho_{max} \leq \rho_*$ and $T_* \leq T_{max} \leq T_\infty$ almost every-where in Ω. Therefore, the limits $(R_{max}, T_{max}, \rho_{max})$ are admissible initial values for the droplet evaporation problem. Theorem 1 thus yields a unique weak solution on $[t_{max}, t_{max} + \varepsilon)$ for some $\varepsilon > 0$. Concatenating the weak solutions on I_{max} and $[t_{max}, t_{max} + \varepsilon)$ defines a weak solution on the extended time interval $[0, t_{max} + \varepsilon)$, which contradicts I_{max} being maximal. Consequently, R_{max} has to be zero. ∎

4. Numerical examples

The following numerical examples illuminate how different air flows around a single spherical droplet affect its evaporation process. For the ease of presentation, we always
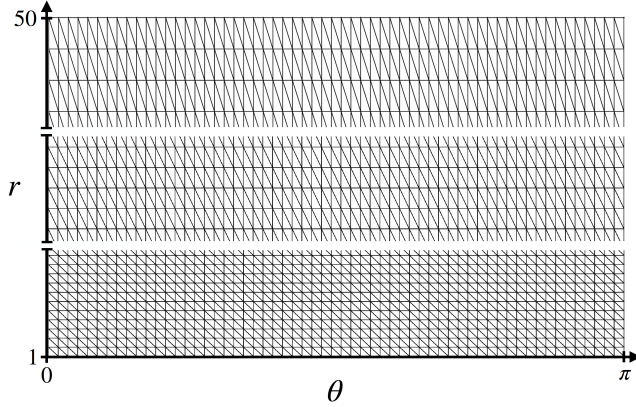
Figure 2. Mesh refinement towards the droplet. Due to the large aspect ratio of our computational domain, only three sections of the mesh are shown. The r-axis is interrupted accordingly.

consider a 1 μl water droplet evaporating at $T_\infty = 60\,°\text{C}$ and $\text{RH}_\infty = 10\,\%$ where $\text{RH}_\infty := \rho_\infty / \rho_{\text{sat}}(T_\infty)$ denotes the relative humidity of the drying air. Other drying conditions are studied in [4, 9, 10] with similar direct numerical simulations. From [10] we also adopt the physical parameters of our model.

The considered air flows will be rotationally symmetric with respect to the vertical axis. Therefore, transforming our single droplet evaporation model into spherical coordinates allows us to neglect the azimuth. Let $\theta \in [0, \pi]$ be the polar angle and $r \geq 0$ the radial distance to the droplet center. Taking into account the aforementioned symmetry, all simulations are performed in the computational domain

$$\Omega = \left\{ (\theta, r) \in \mathbb{R}^2 \, : \, 0 \leq \theta \leq \pi, \, 1 \leq r \leq 50 \right\}, \tag{4.1}$$

representing the two-dimensional generatrix of the rescaled gas phase. We use Gmsh (version 4.4.1) to generate a structured mesh for Ω consisting of 58,882 triangles. As shown in Figure 2, their resolution increases towards the droplet surface. To be more specific, the triangles are successively stretched by 0.25% in each horizontal layer starting from the droplet surface. We then apply the finite element method (FEM) using a semi-implicit Euler scheme to compute the temperature and vapor mass distributions in a monolithic (coupled) manner. Apart from the droplet radius, all unknowns are treated implicitly and Newton's method is applied in each time step. Regarding the accuracy of our numerical results, the uniform time step size $\Delta t = 1\text{s}$ was found to be sufficiently small. Second-order Lagrange elements serve as basis functions for our FEM simulations, which are implemented in C++ with the Distributed and Unified Numerics Environment DUNE [5, 12, 24, 31]. The corresponding linear systems are assembled automatically by

the module dune-fufem[3] from our weak formulations after being linearized and transformed into spherical coordinates. We apply UMFPACK [8] as a direct solver to compute the resulting $237,762$ degrees of freedom. Our numerical results are finally visualized with ParaView (version 5.7.0) after being transformed back into Euclidean coordinates. The resulting images in Figures 3, 4(a), and 5(a) do not show the whole computational domain, but only the interesting area near the droplet.

4.1. Stokes flow

We first consider the evaporation of a spherical droplet exposed to a laminar air flow in the ambient gas phase. The corresponding velocity field is described by the following analytical solution of the Stokes equations [21]:

$$v_\theta = -V_\infty \sin\theta \left(1 - \frac{1}{4r^3} - \frac{3}{4r}\right),$$
$$v_r = V_\infty \cos\theta \left(1 + \frac{1}{2r^3} - \frac{3}{2r}\right),$$

$$(4.2)$$

where v_θ and v_r denote the velocity components in polar and radial direction, respectively. The flow parameter $V_\infty \geq 0$ determines the ambient velocity far away from the droplet. Notice that the required Lipschitz continuity in (2.14) holds, since (4.2) does not even depend on the droplet radius. This is due to the fact that the radial coordinate r is rescaled with the droplet radius. Further notice that (4.2) meets the boundary condition $v_g \cdot n = 0$ on Γ_d required in assumption (A6), since $v_r = 0$ at the droplet surface.

Figure 3(a) illustrates the Stokes flow around the droplet for $V_\infty = 40$ cm/s. The convective impact of the Stokes flow on heat and vapor mass distributions is visualized in Figure 4(a).

One can clearly see that the vapor evaporating from the droplet is blown away in vertical direction. Likewise, the air above the droplet has a lower temperature than the one below or around its equator. Therefore, the evaporation rate increases from the north towards the south pole of the droplet where the normal heat flux assumes its maximum. Recall from Section 1 that the evaporation of a spherical droplet into stagnant air is well described by the d^2 law. According to [9, 10], the d^2 law is given by

$$\frac{dR_d^2}{dt} = -\frac{2k_g(T_\infty - T_d)}{\rho_w \Lambda_w},$$

$$(4.3)$$

together with the implicit equation

$$\frac{\rho_{\text{sat}}(T_d) - \rho_\infty}{T_\infty - T_d} = \frac{k_g}{D_v \Lambda_w}$$

$$(4.4)$$

---

[3]Module description of dune-fufem: https://www.dune-project.org/modules/dune-fufem/

(a) Stokes flow at $V_\infty = 40$ cm/s.
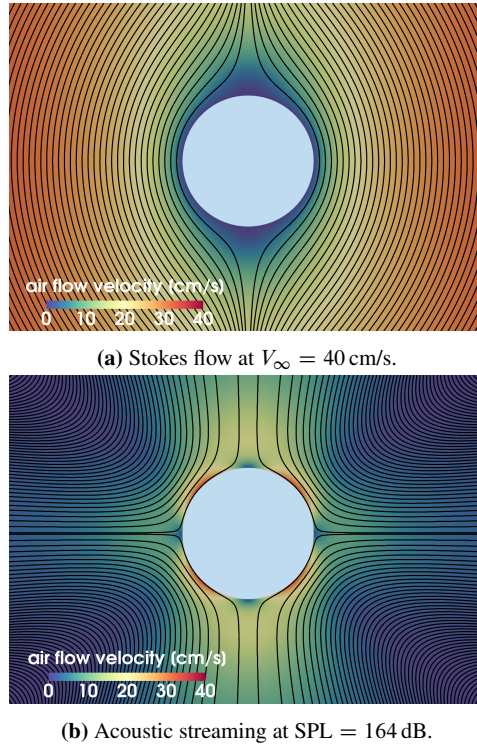

(b) Acoustic streaming at SPL $= 164$ dB.

Figure 3. Air flows around the $1\,\mu$l droplet considered in our numerical examples.

for the uniform temperature T_d of the droplet. Figure 4(b) compares the evolution of the normed squared droplet radius obtained from the d^2 law and our direct numerical simulations. If the latter are performed without convection, both curves coincide almost exactly. Notice that the simulated droplet evaporates slightly faster than predicted by the d^2 law. This is due to the truncation of the gas phase at the rescaled distance $r = 50$ from the droplet center. The Stokes flow, on the other hand, makes the droplet evaporate significantly faster. Depending on the ambient gas velocity, the lifetime of the droplet is reduced by up to 50 %. Furthermore, the normed squared droplet radii are no longer linear but slightly convex. Therefore, the evaporation rate decreases as the droplet becomes smaller.

4.2. Acoustic streaming

Our second numerical example addresses the convection inside an acoustic levitator and requires a brief introduction to understand its physical background. Acoustic leviation is a very elegant way to perform single droplet drying experiments [32]. Avoiding physical contact, a standing ultrasound wave is used to immobilize a single droplet in one of its sound pressure nodes. More precisely, the so-called acoustic radiation pressure counter-
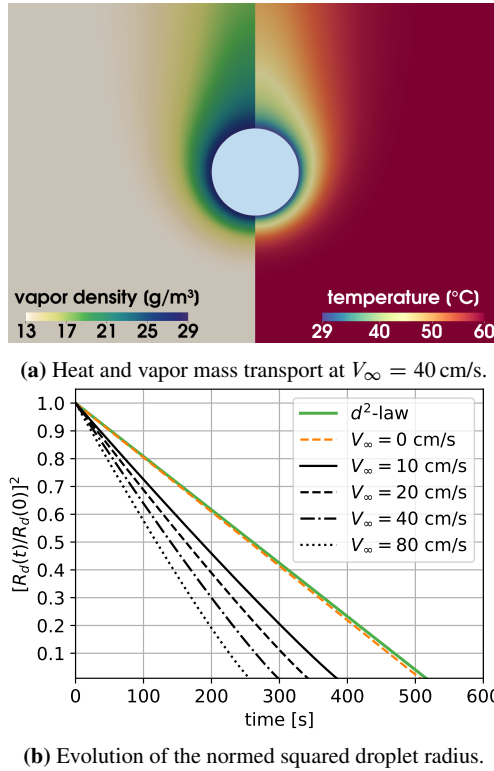
(a) Heat and vapor mass transport at $V_\infty = 40$ cm/s.

(b) Evolution of the normed squared droplet radius.

Figure 4. Convective impact of the Stokes flow on the evaporation process of a $1\,\mu$l water droplet under the drying conditions $T_\infty = 60\,°C$ and $RH_\infty = 10\,\%$.

acts gravity [3]. However, the rapid attenuation of the sound wave at the droplet surface also causes fluid circulations inside the viscous boundary layer. This microscopic effect induces a steady air flow in the ambient gas phase, which is commonly known as outer acoustic streaming [38]. According to [23], its polar and radial components are given by

$$v_\theta = -\frac{45A^2}{32\omega R_d \rho_g^2 c_0^2}\frac{1}{r^4}\sin 2\theta,$$

$$v_r = \frac{45A^2}{32\omega R_d \rho_g^2 c_0^2}\left(\frac{1}{r^2} - \frac{1}{r^4}\right)(3\cos^2\theta - 1),$$

(4.5)

where A denotes the sound pressure amplitude, ω the angular sound frequency, and c_0 the speed of sound in air. It should be pointed out that (4.5) only applies to a spherical droplet whose center lies in one of the sound pressure nodes generated by a planar acoustic levitation wave. Further notice that (4.5) meets the boundary condition $v_g \cdot n = 0$ on Γ_d required in assumption (A6), since $v_r = 0$ at the droplet surface. The sound pressure amplitude A is usually expressed in terms of the corresponding sound pressure level (SPL)
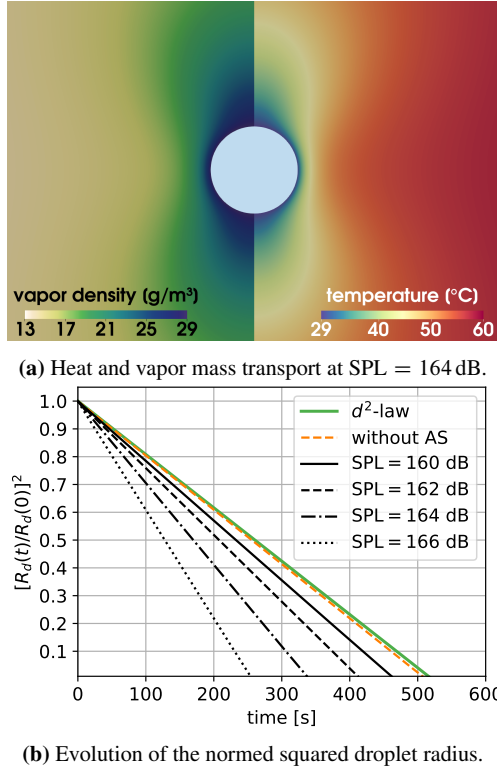
(a) Heat and vapor mass transport at SPL = 164 dB.

(b) Evolution of the normed squared droplet radius.

Figure 5. Convective impact of the acoustic streaming (AS) on the evaporation process of a $1\,\mu l$ water droplet under the drying conditions $T_\infty = 60\,°C$ and $RH_\infty = 10\,\%$.

given by

$$SPL = [20 \cdot \log_{10}(A/Pa) + 94]\ dB \tag{4.6}$$

in decibel [38]. Unlike the Stokes flow in (4.2) considered in Section 4.1, the acoustic streaming now actually depends on the droplet radius. Lipschitz condition (2.14) can be easily verified.

Figure 3(b) illustrates the acoustic streaming around a $1\,\mu l$ droplet levitated at SPL = 164 dB. The corresponding heat and vapor mass distributions in the ambient gas phase are visualized in Figure 5(a).

It can be observed that the vapor evaporating from the droplet is blown away from its equator towards its vertical poles. Likewise, the air above and below the droplet has a lower temperature than the one around its equator. As argued in [10], the evaporation rate increases with the normal heat flux from the vertical poles towards the equator of the levitated droplet. Figure 5(b) compares the evolution of the normed squared droplet radius obtained from the d^2 law and our direct numerical simulations. The small deviation of our simulated curve without the acoustic streaming from the d^2 law was already

discussed before. Like the Stokes flow, the acoustic streaming also accelerates the evaporation process of the levitated droplet. Especially at higher sound pressure levels, the lifetime of the droplet is reduced significantly. As a concluding remark, we mention that the droplet levitated at SPL $= 166\,\mathrm{dB}$ evaporates approximately as fast as the one exposed to the Stokes flow with $V_\infty = 80\,\mathrm{cm/s}$.

5. Conclusion

We successfully applied Banach's fixed-point theorem to study the well-posedness of a coupled ODE–PDE system describing the convective evaporation of a spherical droplet. The decoupled problem (for given droplet radius) was shown to admit a unique weak solution using the method of upper and lower solutions. To address the fully coupled ODE–PDE system, we reformulated it as a fixed-point problem. The underlying Volterra operator for the droplet radius was shown to be a contraction for short time intervals. The unique existence of a maximal weak solution finally followed from a topological argument. Apart from these analytical results, we applied the finite element method to perform direct numerical simulations. The d^2 law was used to validate our numerical results. We visualized the temperature and vapor mass distributions to investigate the convective impact of two different air flows (Stokes flow and acoustic streaming) around the droplet. Both turned out to accelerate its evaporation process.

 Recall that our single droplet evaporation model is limited to several simplifications. Instead of assuming the droplet to be isothermal, it would be physically more accurate to compute its temperature from an additional heat equation. Also, the shape of the droplet could be derived from a balance of forces including surface tension to account for possible deformations. Finally, the air flow in the ambient gas phase should be modeled by the Navier–Stokes equations with a nontrivial convective flux across the droplet surface, taking into account its evolution over time. Extending our model in the aforementioned ways leads to new mathematical challenges that are to be addressed in the future.

A. Appendix

In the following, we derive the upper bound in (3.65) for the sum $d = 2(d_T + d_\rho)$ of the defects in (3.56) and (3.60) containing all products with δR, $\delta \dot{R}$, or δv that appear in the proof of Proposition 2.

Lemma. *The total defect d defined in the proof of Proposition 2 is bounded by*

$$|d| \le \varepsilon(\|\nabla \delta T\|_{2,\Omega}^2 + \|\nabla \delta \rho\|_{2,\Omega}^2) + C\Big[(1 + \|\nabla T_2\|_{2,\Omega}^2 + \|\nabla \rho_2\|_{2,\Omega}^2)\delta R^2$$

$$+ \frac{1}{\varepsilon}(\delta \dot{R}^2 + \|\delta T\|_{2,\Omega}^2 + \|\delta \rho\|_{2,\Omega}^2)\Big] \qquad (*)$$

with $\varepsilon > 0$ being arbitrarily small.

Proof. Recall $|\delta T| \leq T_\infty - T_*$, $|\delta \rho| \leq \rho_* - \rho_\infty$, and $|J_2| \leq J_\infty$ due to lower and upper bounds (3.27) from Proposition 1. Assumption (A6) further implies $\|\delta v\|_{\infty,\Omega} \leq C|\delta R|$ and $\|v_2\|_{\infty,\Omega} \leq C$. Therefore, the individual terms of the temperature defect in (3.56) can be handled as follows:

$$\int_\Omega \delta R(\nabla T_2 \cdot v_2)\delta T \, dx \leq C|\delta R|\|\nabla T_2\|_{2,\Omega}\|\delta T\|_{2,\Omega} \leq C(\delta R^2\|\nabla T_2\|_{2,\Omega}^2 + \|\delta T\|_{2,\Omega}^2),$$

$$-\int_\Omega R_2(\nabla T_2 \cdot \delta v)\delta T \, dx \leq C|\delta R|\|\nabla T_2\|_{2,\Omega}\|\delta T\|_{2,\Omega} \leq C(\delta R^2\|\nabla T_2\|_{2,\Omega}^2 + \|\delta T\|_{2,\Omega}^2),$$

$$-\int_\Omega \delta R \dot{R}_2(\nabla T_2 \cdot x)\delta T \, dx \leq C|\delta R|\|\nabla T_2\|_{2,\Omega}\|\delta T\|_{2,\Omega} \leq C(\delta R^2\|\nabla T_2\|_{2,\Omega}^2 + \|\delta T\|_{2,\Omega}^2),$$

$$\int_\Gamma \delta R J_2 \delta T \, d\sigma \leq C(\delta R^2 + \|\delta T\|_{2,\Gamma}^2)$$

$$\leq \varepsilon\|\nabla\delta T\|_{2,\Omega}^2 + C\left(\delta R^2 + \frac{1}{\varepsilon}\|\delta T\|_{2,\Omega}^2\right), \qquad (**)$$

$$\int_\Omega \delta R \nabla T_2 \cdot \nabla\delta T \, dx \leq |\delta R|\|\nabla T_2\|_{2,\Omega}\|\nabla\delta T\|_{2,\Omega} \leq \varepsilon\|\nabla\delta T\|_{2,\Omega}^2 + \frac{C}{\varepsilon}\delta R^2\|\nabla T_2\|_{2,\Omega}^2$$

using Hölder's and Young's inequalities. Notice that the last inequality in $(**)$ follows from Lemma 1. The temperature defect term involving $\delta\dot{R}$ is somewhat more delicate and thus treated separately. First of all, we apply the divergence theorem to compute

$$-\int_\Omega R_2\delta\dot{R}(\nabla T_2 \cdot x)\delta T \, dx = 3\int_\Omega R_2\delta\dot{R}T_2\delta T \, dx + \int_\Gamma R_2\delta\dot{R}T_2\delta T \, d\sigma$$
$$+ \int_\Omega R_2\delta\dot{R}T_2(\nabla\delta T \cdot x) \, dx,$$

taking into account $\nabla T_2 \cdot x = \nabla \cdot (T_2 x) - 3T_2$ in Ω and $x \cdot n = -1$ on Γ. The estimate

$$-\int_\Omega R_2\delta\dot{R}(\nabla T_2 \cdot x)\delta T \, dx \leq \varepsilon\|\nabla\delta T\|_{2,\Omega}^2 + \frac{C}{\varepsilon}(\delta\dot{R}^2 + \|\delta T\|_{2,\Omega}^2)$$

then follows from Young's inequality and Lemma 1. Altogether, we obtain the upper bound

$$|d_T| \leq \varepsilon\|\nabla\delta T\|_{2,\Omega}^2 + C\left[(1 + \|\nabla T_2\|_{2,\Omega}^2)\delta R^2 + \frac{1}{\varepsilon}(\delta\dot{R}^2 + \|\delta T\|_{2,\Omega}^2)\right]$$

for the temperature defect. Likewise, we obtain a similar upper bound for the vapor mass defect

$$|d_\rho| \leq \varepsilon\|\nabla\delta\rho\|_{2,\Omega}^2 + C\left[(1 + \|\nabla\rho_2\|_{2,\Omega}^2)\delta R^2 + \frac{1}{\varepsilon}(\delta\dot{R}^2 + \|\delta\rho\|_{2,\Omega}^2)\right],$$

using the same arguments as before. The upper bound given by $(*)$ for the total defect $d = 2(d_T + d_\rho)$ then follows from the previous estimates for d_T and d_ρ via summation. ∎

Nomenclature

Ω gas phase

Γ droplet surface

Γ_∞ outer boundary of the gas phase

R droplet radius

T gas temperature

T_∞ gas temperature of the drying air

ρ vapor mass density

ρ_∞ vapor mass density of the drying air

ρ_{sat} saturated vapor mass density

J evaporation rate

v air flow velocity

References

[1] R. A. Adams, *Sobolev spaces*. Pure and Applied Mathematics 65, Academic Press, New York-London, 1975 Zbl 0314.46030 MR 450957

[2] D. M. Anderson, P. Cermelli, E. Fried, M. E. Gurtin, and G. B. McFadden, General dynamical sharp-interface conditions for phase transformations in viscous heat-conducting fluids. *J. Fluid Mech.* **581** (2007), 323–370 Zbl 1119.76066 MR 2333066

[3] M. Andrade, N. Pérez, and J. Adamowski, Review of progress in acoustic levitation. *Braz. J. Phys* **48** (2018), 190–213

[4] E. Bänsch and M. Götz, Numerical study of droplet evaporation in an acoustic levitator. *Phys. Fluids* **30** (2018), no. 3, article no. 037103

[5] P. Bastian, M. Blatt, A. Dedner, N.-A. Dreier, C. Engwer, R. Fritz, C. Grüninger, D. Kempf, R. Klöfkorn, M. Ohlberger, and O. Sander, The Dune framework: basic concepts and recent developments. *Comput. Math. Appl.* **81** (2021), 75–112 Zbl 1524.65003 MR 4189803

[6] C. Beckermann and R. Viskanta, Mathematical modeling of transport phenomena during alloy solidification. *AMR* **46** (1993), no. 1, 1–27 MR 1198518

[7] C. Borgnakke and R. Sonntag, *Fundamentals of thermodynamics*. 7th edn., Wiley, 2009

[8] T. A. Davis, Algorithm 832: UMFPACK V4.3—an unsymmetric-pattern multifrontal method. *ACM Trans. Math. Software* **30** (2004), no. 2, 196–199 Zbl 1072.65037 MR 2075981

[9] M. Doß and E. Bänsch, Numerical study of single droplet drying in an acoustic levitator before the critical point of time. *Chem. Eng. Sci.* **248** (2022), article no. 117149

[10] M. Doß, N. Ray, and E. Bänsch, Modeling and simulation of single droplet drying in an acoustic levitator. *Drying Technology* **41** (2023), no. 13, 2088–2104

[11] J. Escher, J. Prüss, and G. Simonett, Analytic solutions for a Stefan problem with Gibbs-Thomson correction. *J. Reine Angew. Math.* **563** (2003), 1–52 Zbl 1242.35220 MR 2009238

[12] C. Engwer and S. Müthing, Concepts for flexible parallel multi-domain simulations. In *Domain decomposition methods in science and engineering XXII*, ed. T. Dickopf et al., pp. 187–195. Lect. Notes Comput. Sci. Eng. 104, Springer, Cham, 2016 Zbl 1338.65262 MR 3643553

[13] L. C. Evans, *Partial differential equations*. Second edn., Grad. Stud. Math. 19, American Mathematical Society, Providence, RI, 2010 Zbl 1194.35001 MR 2597943

[14] A. Friedman, Free boundary problems for parabolic equations. II. Evaporation or condensation of a liquid drop. *J. Math. Mech.* **9** (1960), 19–66 Zbl 0091.09302 MR 144079

[15] A. Friedman, Analyticity of the free boundary for the Stefan problem. *Arch. Rational Mech. Anal.* **61** (1976), no. 2, 97–125 Zbl 0329.35034 MR 407452

[16] M. Gahn and I. S. Pop, Homogenization of a mineral dissolution and precipitation model involving free boundaries at the micro scale. *J. Differential Equations* **343** (2023), 90–151 Zbl 1505.35026 MR 4497302

[17] S. Gärttner, P. Knabner, and N. Ray, Local existence of strong solutions to micro-macro models for reactive transport in evolving porous media. *European J. Appl. Math.* **35** (2024), no. 1, 127–154 MR 4686285

[18] M. Herz, *Mathematical modeling and analysis of electrolyte solutions*. PhD thesis, Friedrich-Alexander-Universität Erlangen-Nürnberg, 2014

[19] R. Hołyst, M. Litniewski, and D. Jakubczyk, A molecular dynamics test of the Hertz-Knudsen equation for evaporating liquids. *Soft Matter* **11** (2015), 7201–7206

[20] O. A. Ladyženskaja, V. A. Solonnikov, and N. N. Ural'ceva, *Linear and quasilinear equations of parabolic type*. Translated from the Russian by S. Smith. *Transl. Math. Monogr.* 23, American Mathematical Society, Providence, RI, 1968 MR 241822

[21] L. D. Landau and E. M. Lifshitz, *Fluid mechanics*. Translated from the Russian by J. B. Sykes and W. H. Reid. Second edn. Course of Theoretical Physics 6, Pergamon Press, London-Paris-Frankfurt; Addison-Wesley Publishing Company, Reading, MA, 1987 Zbl 0655.76001

[22] C. Law, *Combustion physics*. Cambridge University Press, 2006

[23] C. Lee and T. Wang, Outer acoustic streaming. *J. Acoust. Soc. Am* **88** (1990), no. 5, 2367–2375

[24] C. Engwer, C. Gräser, S. Müthing, and O. Sander, The interface for functions in the dune-functions module. *Archive of Numerical Software* **5** (2017), no. 1, 95–109

[25] F. Murray, On the computation of saturation vapor pressure. *Journal of Applied Meteorology and Climatology*. **6** (1967), no. 1, 203–204

[26] C. V. Pao, *Nonlinear parabolic and elliptic equations*. Plenum Press, New York, 1992 Zbl 0777.35001 MR 1212084

[27] K. Patel, X. Chen, and S. Kar, The temperature uniformity during air drying of a colloidal liquid droplet. *Drying Technology* **23** (2005), no. 12, 2337–2367

[28] J. Prüss and S. Shimizu, On well-posedness of incompressible two-phase flows with phase transitions: the case of non-equal densities. *J. Evol. Equ.* **12** (2012), no. 4, 917–941 Zbl 1259.35226 MR 3000462

[29] J. Prüss and S. Shimizu, Y. Shibata, and G. Simonett, On well-posedness of incompressible two-phase flows with phase transitions: the case of equal densities. *Evol. Equ. Control Theory* **12** (2012), no. 1, 171–194 Zbl 1302.76066 MR 3085224

[30] L. I. Rubenšteĭn, *The Stefan problem*. Transl. Math. Monogr. 27, American Mathematical Society, Providence, RI, 1971 Zbl 0208.09804 MR 351348

[31] O. Sander, *DUNE—the distributed and unified numerics environment*. Lect. Notes Comput. Sci. Eng. 140, Springer, Cham, 2020 Zbl 1483.65004 MR 4221187

[32] H. Schiffter and G. Lee, Single-droplet evaporation kinetics and particle formation in an acoustic levitator. part 1: Evaporation of water microdroplets assessed using boundary-layer and acoustic levitation theories. *Journal of Pharmaceutical Sciences* **96** (2007), no. 9, 2274–2283

[33] S. Semenov, V. Starov, M. Velarde, and R. Rubio, Droplets evaporation: Problems and solutions. *EPJ - Special Topics* **197** (2011), 265–278

[34] R. Vehring, Pharmaceutical particle engineering via spray drying. *Pharmaceutical research* **25** (2008), 999–1022

[35] A. Visintin, Introduction to Stefan-type problems. In *Handbook of differential equations: evolutionary equations. Vol. IV*, pp. 377–484, Handb. Differ. Equ., Elsevier/North-Holland, Amsterdam, 2008 Zbl 1183.35279 MR 2508170

[36] K. Wang and R. Dickinson, A review of global terrestrial evapotranspiration: Observation, modeling, climatology, and climatic variability. *Rev. Geophys.* **50** (2012), no. 2, article no. RG2005

[37] J. Wloka, *Partial differential equations*. Cambridge University Press, Cambridge, 1987 Zbl 0623.35006 MR 895589

[38] A. Yarin, G. Brenn, O. Kastner, D. Rensink, and C. Tropea, Evaporation of acoustically levitated droplets. *J. Fluid Mech.* **399** (1999), 151–204 Zbl 0982.76092

[39] M. Zientara, D. Jakubczyk, M. Litniewski, and R. Hołyst, Transport of mass at the nanoscale during evaporation of droplets: the Hertz-Knudsen equation at the nanoscale. *J. Phys. Chem. C* **117** (2013), no. 2, 1146–1150

Eberhard Bänsch
Department of Mathematics, Friedrich-Alexander University Erlangen-Nürnberg, Cauerstraße 11, 91058 Erlangen, Germany; baensch@math.fau.de

Martin Doß
Department of Mathematics, Friedrich-Alexander University Erlangen-Nürnberg, Cauerstraße 11, 91058 Erlangen, Germany; martin.doss@math.fau.de

Carsten Gräser
Department of Mathematics, Friedrich-Alexander University Erlangen-Nürnberg, Cauerstraße 11, 91058 Erlangen, Germany; graeser@math.fau.de

Nadja Ray
Department of Mathematics, Friedrich-Alexander University Erlangen-Nürnberg, Cauerstraße 11, 91058 Erlangen; Mathematical Institute for Machine Learning and Data Science, Catholic University Eichstätt–Ingolstadt, Hohe-Schul-Straße 5, 85049 Ingolstadt, Germany; nadja.ray@ku.de